Vortex-antivortex unbinding in inhomogeneous 2D atomic condensates

Journal of Low Temperature Physics manuscript No.
(will be inserted by the editor)

J. Tempere, S. Driezen, W. Van Alphen, E. Lories, E. Vermeyen

Vortex-Antivortex unbinding in inhomogeneous 2D atomic condensates

25.06.2013

Keywords Bose-Einstein Condensate, Vortices, Kosterlitz-Thouless
Abstract The breakdown of superfluidity in a two-dimensional Bose gas is linked with the unbinding of vortex-antivortex pairs, which has been observed directly in a recent experiment with trapped atomic gases. The phenomenological Kosterlitz-Thouless description of the dissociation process, originally set up in the context of a uniform Bose system (such as superfluid helium), is no longer suited in the case of a strongly inhomogenous atomic gas in which, moreover, the vortex core size is a non-negligible fraction of the cloud size. Using the Gross-Pitaevskii energy functional we extend the original Kosterlitz-Thouless argument to take into account inhomogeneity and vortex core size in the calculation of both the binding energy of the vortex-antivortex pair, and the entropy per vortex in the cloud. We derive the resulting shift in the Kosterlitz-Thouless temperature, and find that it is in good agreement with experiment, in contrast to the value obtained in the context of the uniform Bose gas. Finally, we look at different intermediate levels of approximation for the binding energy and the entropy and investigate their effect on the shift in the Kosterlitz-Thouless temperature.

PACS numbers: 03.75.Hh,03.75.Kk,67.85.De

1 Introduction

Vortex-antivortex pairs lie at the heart of the description of superfluidity in two dimensions (2D) [1]. The Kosterlitz-Thouless (KT) mechanism whereby superfluidity is lost in 2D is the unbinding of these vortex-antivortex pairs [2,3,4,5]. Above the BKT temperature T_{KT} the entropic contribution to the free energy overcomes the binding energy of the pair. As a result, free vortices and antivortices proliferate, destroying the phase coherence without which superfluidity is impossible.

TQC, Universiteit Antwerpen, Universiteitsplein 1, B-2610 Antwerpen, Belgium
E-mail: jacques.tempere@ua.ac.be

In a recent experiment, the BKT mechanism was observed in a tightly confined 2D atomic Bose gas cooled to nanokelvin temperatures[6,7]. Dissociated vortex-antivortex pairs were revealed by matter-wave interferometry as they produce a tell-tale dislocation in the fringe pattern. Counting the number of these dislocations directly provides the number of dissociated vortex-antivortex pairs. This was studied as a function of temperature, which in turn was determined from the fringe contrast. The result of this experiment is that above a given temperature, estimated at 290 ± 40 nK, the number of dissociated vortex-antivortex pairs suddenly and rapidly increases. Once free, the vortices and antivortices move to the edge of the cloud, along a preferred direction related to the easy axis of the elliptic cloud.

The temperature at which this occurs is found to be lower than the predicted BKT temperature based on the central density of the cloud and its temperature. This is not suprising, since the derivation is for a homogenous 2D Bose gas in the limit of vanishing core sizes, whereas the realistic system is quite finite and has a healing length that, albeit a factor 30 smaller than the cloud radius, may still play a role. In that respect, the quantum gases are quite different from the case of superfluid ^{4}He where the vortex core size is negligible and the density is to a very good approximation constant. Subsequent Monte-Carlo simulations of great sophistication have since then brought theory in much better agreement with the quantum gas experiments[8,9]. These, and other theoretical investigations[10,11,12,13], focus in essence on the decay of the single particle Green's function and on correlation functions to determine the presence of superfluidity.

Nevertheless we feel the need for a simpler framework in which to phenomenologically understand the effects of condensate confinement and inhomogeneity, akin to the straightforward Kosterlitz-Thouless free energy balance argument for dissociation of vortex-antivortex pairs. Indeed, what the experiment observes is precisely this dissociation and proliferation of vortices and antivortices, rather than the single particle spectrum. The present contribution is born from this desire to set up such a simpler picture. We start from the Gross-Pitaevskii (GP) treatment[14] and show how the confinement leads to an effective radius for dissociation of the vortex-antivortex pair, and to a change in the binding energy of the pair as a function of the ratio of the healing length to the cloud size. The inhomogeneity also results in a change in the entropy per vortex. We show that taking into account these changes in the calculation of the BKT temperature results in a value that is in agreement with the experiment. We peel off some remaining layers of complexity, to see how far we can further simplify the approach and still obtain reasonable results. First, we only take the kinetic energy of the superflow into account in the GP energy functional, dropping all other contributions. Next, we replace even this by a simple formula derived from the Magnus forces on the vortices. From this we can show that although the treatment based only on estimating the Magnus forces gives a good result for the dissociation radius, it does not find the correct binding energies. The Gross-Pitaevskii kinetic energy of the superflow, which takes into account the finite size of the core, is necessary to obtain also quantitative agreement.

2 Gross-Pitaevskii treatment

2.1 Variational energy functional

The Gross-Pitaevskii energy functional

$$E[\Psi(\mathbf{x}),N] = \int d\mathbf{x} \left\{ \frac{\hbar^2}{2m} |\nabla\Psi(\mathbf{x})|^2 + \frac{1}{2} m\omega^2 x^2 |\Psi(\mathbf{x})|^2 + \frac{1}{2} g |\Psi(\mathbf{x})|^4 \right\} \quad (1)$$

can be treated as a variational energy functional for the condensate wave function $\Psi(\mathbf{x})$. Here, the N atoms of mass m are confined by a parabolic potential with frequency ω, and interact through a contact potential with strength g. In the Thomas-Fermi regime, the density of the condensate without vortex is given by

$$\rho_{TF}(\mathbf{x}) = \rho_c \left(1 - \frac{x^2}{R_{TF}^2} \right) \quad (2)$$

where R_{TF} is the size of the cloud and ρ_c is the density at the center of the trap[14]. With this density and the interaction strength, a corresponding healing length

$$\xi_c^{-2} = mg\rho_c/\hbar^2 \quad (3)$$

is defined. We will use this Thomas-Fermi profile as a background density, to be modified by a variational function that introduced a vortex at a given position. For this purpose we substitute

$$\Psi(\mathbf{x}) = \sqrt{\rho_{TF}(\mathbf{x})} f(\mathbf{x}/R_{TF}) e^{i\theta(\mathbf{x})} \quad (4)$$

in the Gross-Pitaevskii functional. Note that the length of the position vector in the variational trial function $f(\mathbf{r})$ is rescaled so that $r = x/R_{TF} = 1$ corresponds to the edge of the Thomas-Fermi cloud. Far away from any vortex, we have $f(\mathbf{r}) = 1$, and $f(\mathbf{r})$ goes to zero as r approaches the position of any vortex core. The phase gradient gives rise to a superfluid velocity, expressed in dimensionless form as

$$\mathbf{v}(\mathbf{r}) = \nabla_{\mathbf{r}} \theta(\mathbf{r} R_{TF}). \quad (5)$$

The dimensionfull superfluid velocity is related to this $\mathbf{v}(\mathbf{r})$ through $\mathbf{v}_s(\mathbf{x}) = [\hbar/(mR_{TF})]\,\mathbf{v}(\mathbf{x}/R_{TF})$. We have written the variational trial function in this particular scaling, since the variational energy now turns into an insightful form:

$$\begin{aligned} E[\Psi(\mathbf{r}),N] = \frac{\hbar^2\rho_c}{2m} \int_{|\mathbf{r}|<1} d\mathbf{r} \Big\{ \left(1-r^2\right) \left[|\nabla_{\mathbf{r}} f(\mathbf{r})|^2 + f^2(\mathbf{r}) \mathbf{v}^2(\mathbf{r}) \right] \\ + \frac{1}{\zeta_c^2} \left[2r^2 \left(1-r^2\right) f^2(\mathbf{r}) + \left(1-r^2\right)^2 f^4(\mathbf{r}) \right] \Big\}. \end{aligned} \quad (6)$$

The energy scale is given by $\hbar^2\rho_c/(2m)$, and the unique control parameter is

$$\zeta_c = \xi_c/R_{TF}, \quad (7)$$

the ratio of the central healing length to the Thomas-Fermi radius. The first line in (6) contains the quantum pressure and the kinetic energy related to the superfluid velocity field, whereas the second line contains the potential energy of the trap and the interaction energy.

In the experiment, usually one reports the number of trapped particles N, the harmonic oscillator trap length a_{HO} and the radius of the cloud R_{TF} (or the peak density ρ_c). From these, we easily obtain the parameters needed for the current formulation:

$$\zeta_c = \sqrt{2}\left(\frac{a_{HO}}{R_{TF}}\right)^2 \tag{8}$$

and

$$\rho_c = 2\frac{N}{\pi R_{TF}^2} \tag{9}$$

Some typical values can be extracted from the ENS experiment[6] on the Kosterlitz-Thouless transition: there one has $N = 11000$ particles, $\rho_c = 5\times 10^9$ cm^{-2} (equivalent to $R_{TF} = 12$ μm), and a geometrical average $a_{HO} = 1.75$ μm, leading to $\zeta_c = 0.03$. In our current treatment, we use an isotropic 2D trapping, but proper rescaling should allow to treat anisotropically trapped (elliptic) 2D systems. Note that the Thomas-Fermi ansatz that we made here breaks down when ζ_c becomes of order 1. So, although for the ENS experiment parameters, we can use the Thomas-Fermi density, for 2D systems with smaller numbers of particles (typically ¡1000) the background density of the condensate may differ from the inverted parabola profile.

2.2 Variational trial function for vortices

The variational trial function for $f(\mathbf{r})$ should drill vortex cores at the positions $\mathbf{r}_j$ of the N_{vor} vortices. For this purpose we choose

$$f(\mathbf{r}) = \prod_{j=1}^{N_{vor}} \tanh\left(\alpha_j \left|\mathbf{r}-\mathbf{r}_j\right|\right) \tag{10}$$

where α_j is an adaptable parameter, fixed variationally. We found that the numerical value corresponds to the analytical value that we obtain for a homogenous condensate, using the local density approximation (good when $\zeta_c \ll 1$):

$$\alpha_j = \frac{1}{\zeta_c}\sqrt{1-r_j^2}\sqrt{\frac{4\ln(2)-1}{3}} \tag{11}$$

Note that as the vortex is located further away from the origin (r_j increases), it is located in regions of lower density and the variational size of the core (roughly α_j^{-1}) increases. Only near the edge of the condensate, where the Thomas-Fermi approximation already fails for the background density, should we expect deviations.

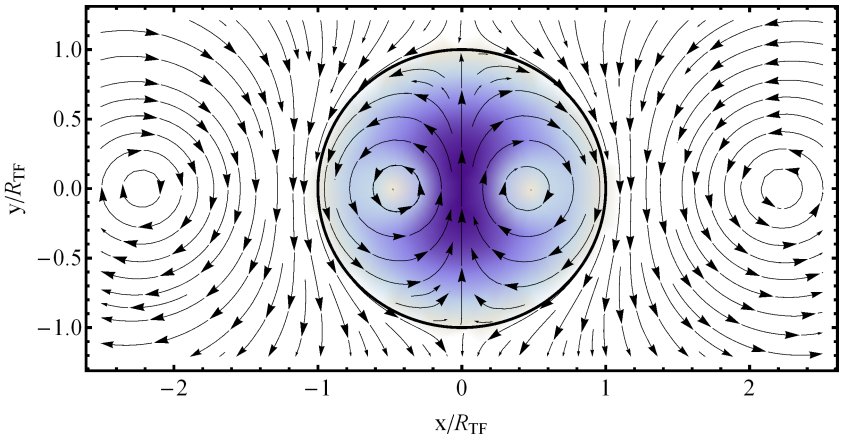

Fig. 1 (Color online) The velocity field streamlines are shown for a condensate with a vortex-antivortex pair. The condensate is confined to the black circle, where the shading inside the circle shows the condensate density from light (low density) to dark (high density). Only the streamlines inside the circle correspond to real superfluid flow that contributes to the kinetic energy. Outside of the condensate, an image vortex and image antivortex are positioned so as to ensure that no superflow crosses the condensate boundary.

The corresponding velocity field is given by

$$\mathbf{v}(\mathbf{r}) = \sum_{j=1}^{N_{vor}} n_j \frac{\mathbf{e}_z \times (\mathbf{r} - \mathbf{r}_j)}{\left|\mathbf{r} - \mathbf{r}_j\right|^2} \tag{12}$$

where we assume $\mathbf{e}_z$ to be orthogonal to the plane of the 2D condensate, and $n_j = +1, -1$ for vortices and antivortices respectively. Here we will look at the case with $N_{vor} = 2$ vortices, of opposite vorticity. This velocity field is suitable for an infinite system: when boundaries are present, it needs to be modified. This can be done by introducing image vortices, as explained below. First, note that when we remove condensate from the vortex core, this condensate density should be relocated elsewhere in order to keep the total number of atoms fixed. This leads in principle to a slight increase in R_{TF}:

$$R_{TF} \to R_{TF} \times \left(1 + \frac{1}{\pi} \int\limits_{|\mathbf{r}|<1} d\mathbf{r} \left(1 - r^2\right) \left[1 - f^2(\mathbf{r})\right] \right) \tag{13}$$

We have checked that for the cases reported here (small ζ_c), the Thomas-Fermi radius does not increase significantly when working with fixed number of atoms, and this effect does not influence the results.

In order to study vortex-antivortex unbinding, we place a vortex at position $\mathbf{r} = r_v \mathbf{e}_x$ and an antivortex in $-\mathbf{r}$, and study the variational energy as a function of r_v. However, care must be taken that the velocity field does not lead to a current that crosses the Thomas-Fermi radius: our variational trial function should satisfy the condition that no atoms flow out of the condensate. This can be achieved using

the method of images. Image vortices are introduced to modify the velocity field near the edges of the condensate: with a vortex in (unscaled) position $\mathbf{x}$ an image anti-vortex is associated at a distance R_{TF}^2/x from the center, also in the direction of $\mathbf{x}$. In our scaled variable, this means that the vortex in $\mathbf{r} = r_v \mathbf{e}_x$ is accompanied by an image antivortex in $\mathbf{r} = (1/r_v)\mathbf{e}_x$. Similarly, the antivortex in $\mathbf{r} = -r_v \mathbf{e}_x$ leads to an image vortex in $\mathbf{r} = (-1/r_v)\mathbf{e}_x$. The resulting flow pattern is illustrated in figure 1, along with the density profile.

3 Dissociation radius and binding energy

In order to study the binding energy of a vortex-antivortex pair in the trapped condensate, we track the evolution of the energy as the pair is pulled apart. For this purpose, we start with a vortex and antivortex touching eachother at a distance $r_v = \zeta_c$, and plot the variational energy (6) as r_v is increased towards 1. The result is shown in figure 2, for the specific case where $\zeta_c = 0.03$. In the variational velocity profile (12), we have included the required image vortices.

Not all the different contributions to the energy matter. It is clear that the quantum pressure (lower inset, long dashed curve) is small, as it should be in the Thomas-Fermi regime. But also the sum of the potential energy of the trap (upper inset, dash-dotted curve) and the interaction energy of the condensate (upper inset, dashed curve) does not depend strongly on the position of the vortex. Both contributions are related to the fact that we need to remove condensate atoms from the vortex core. When the vortex is moved to the edge, the core area (the local healing length squared) grows inversely proportional to the local density. Nevertheless, the number of atoms removed from the core stays roughly constant, as this is the product of local density with core area. So, although the sum of the potential and interaction energy is large, it does not contribute strongly to the *change* of the total energy as we move vortices to the edge of the condensate comes. The main contribution to the energy gradient comes from the kinetic energy of the superfluid flow (E_{SF}, full curve in the main graph of figure 2).

The total energy, as well as the kinetic energy of the superfluid velocity field has a maximum as a function of the position of the vortex as it is pulled apart from the antivortex. The maximum occurs at $r_c \approx 0.282$, for $\zeta_c = 0.03$. This means that for distances $r < r_c$, the vortex is pulled back to the antivortex, and both recombine at the center of the trap. For distances $r > r_c$, the vortex is pulled to towards the edge of the cloud, and the vortex-antivortex molecule dissociates. Therefore, we refer to this radius r_c as the "dissociation radius" of the vortex-antivortex pair in the trapped condensate.

The existence of such a dissociation radius can be understood from the point of view of Magnus forces acting on the vortex. The vortex at $\mathbf{r}_v = r_v \mathbf{e}_x$, with circulation κ, finds itself in the velocity field $\mathbf{v}(\mathbf{r}_v)$ generated by the antivortex and the two image vortices. If the vortex is treated as a point object (in 2D), the force acting on it is $\mathbf{F} = m\rho_c \kappa \times \mathbf{v}$. Summing up the contributions from the antivortex (at a distance $2r_v$ from the vortex), the image antivortex (at a distance $r_v^{-1} - r_v$ and the image vortex (at a distance $r_v^{-1} + r_v$), we get a force directed along the

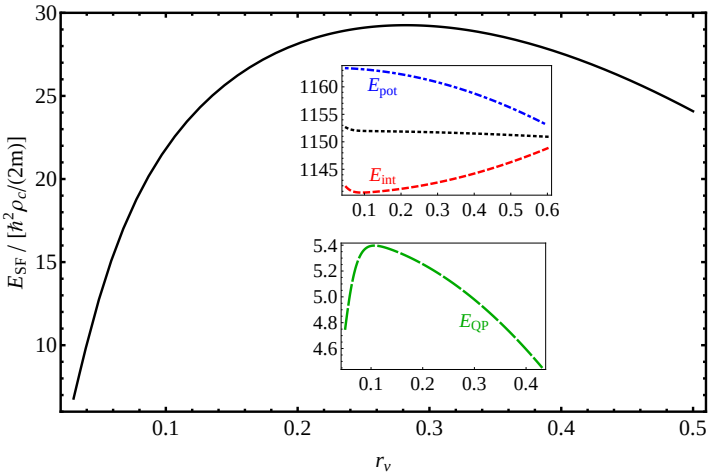

Fig. 2 (Color online) The contributions to the variational energy of a vortex-antivortex pair are shown as a function of the distance of the vortex (and antivortex) from the center of the trap, cf. the setup in figure 1. In the insets, the dashed curve labeled E_{int} is the interaction energy, the dash-dotted curve labeled E_{pot} is the potential energy related to the trapping potential, the dotted curve is the average of E_{int} and E_{pot}, and the long dashed curve labeled E_{QP} is the quantum pressure. The main graph shows E_{SF}, the kinetic energy related to the superfluid velocity field. All energies are in units $\hbar\rho_c/(2m)$, and all energies are plotted as a function of the distances in units R_{TF}. These curves were generated for $\xi/R_{TF} = 0.03$.

x-direction:

$$F_x = 4\pi\frac{\hbar^2\rho_c}{2m}\left(-\frac{1}{2r_v}+\frac{1}{r_v^{-1}-r_v}+\frac{1}{r_v^{-1}+r_v}\right)$$
$$= -2\pi\frac{\hbar^2\rho_c}{2m}\frac{r_v^4+4r_v^2-1}{r_v\,(r_v^4-1)} \tag{14}$$

The vortex is in equilibrium for

$$F_x = 0 \Leftrightarrow r_v = r_c = \sqrt{\sqrt{5}-2} = 0.486... \tag{15}$$

For distances larger than r_c, the pull of the image antivortex towards the edge of the cloud is stronger than the pull of the (real) antivortex towards the center, and the vortex-antivortex molecule dissociates. Our calculations based on the Magnus force for point vortices gives insight into the existence of the dissociation radius, but differs quantitatively from the more precise calculation using the GP variational energy in a finite condensate.

The binding energy E_b can now be calculated as the energy required to pull a vortex and an antivortex apart up to the dissociation radius:

$$E_b = E_{SF}(r_v = r_c) - E_{SF}(r_v = \zeta_c). \tag{16}$$

The result, as a function of $1/\zeta_c = R_{TF}/\xi_c$, is shown in figure 3. On the basis of the Magnus forces outlined above, expression (14), we can get an approximate but

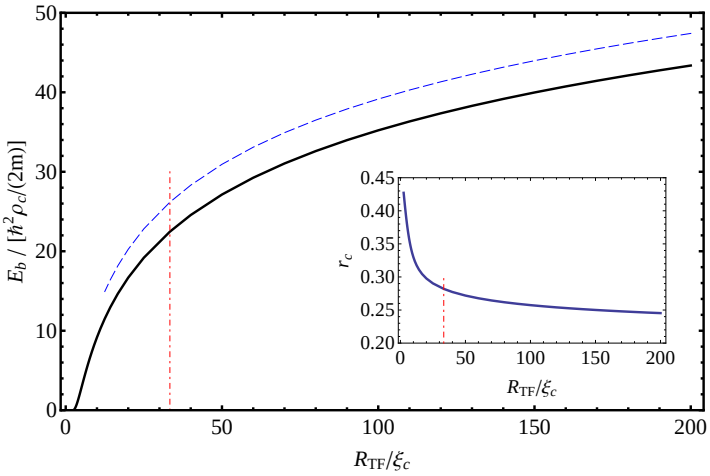

Fig. 3 (Color online) The binding energy of a vortex-antivortex pair is shown as a function of the size of the (parabolically trapped) condensate, expressed through R_{TF}/ξ_c. In the inset, the corresponding dissociation radius r_c is shown: when vortex and antivortex are pulled further apart this distance (in units R_{TF}), the pair dissociates and vortices move to the edge of the cloud. The dash-dotted vertical line shows the value of R_{TF}/ξ_c estimated for the experiment of Hadzibabic *et al.*[6]. The dashed curve represents the approximate result based on Magnus forces acting on point vortices, and the full curve is the result based on the GP variational energy.

analytic result by integrating $F_x(r_v)$ from ζ_c to r_c :

$$E_b^{magn} = 4\pi \left[\log\left(\frac{r_c(1-r_c^2)}{1+r_c^2} \right) + \log\left(\frac{(1+\zeta_c^2)}{\zeta_c(1-\zeta_c^2)} \right) \right]. \tag{17}$$

This result is shown as the dashed curve in figure 3. As R_{TF}/ξ_c increases, the relative difference between this approximate expression and the result obtained from the GP equation diminishes. Moreover, since r_c goes to a fixed fraction of R_{TF}, we find that this equation reproduces the KT result for a homogeneous Bose gas, with homogeneous density ρ_c, in the limit of radius approaching infinity: $E_b^{KT} = -4\pi\log(\zeta_c)$. However, for $\zeta = 0.03$ there is still a strong difference: in our units, $E_b^{KT} \approx 44.1$, $E_b^{magn} \approx 26.2$ and $E_b \approx 22.5$. This difference, due to the finite size and inhomogeneity of the condensate, will lead to a difference in the expected temperature at which vortices and antivortices unbind. To find this temperature, we still need to investigate the effects of the finite size and inhomogeneity on the entropy.

4 Vortex entropy in an inhomogeneous condensate

In the original KT argument, the binding energy $E_b^{KT} = -4\pi\log(\zeta_c)$ is balanced by the thermal contribution TS where T is the temperature and S the entropy. The entropy is estimated by taking the logarithm of the number of (microscopic) ways of placing the vortex and the antivortex in the condensate. For objects of size ξ_c

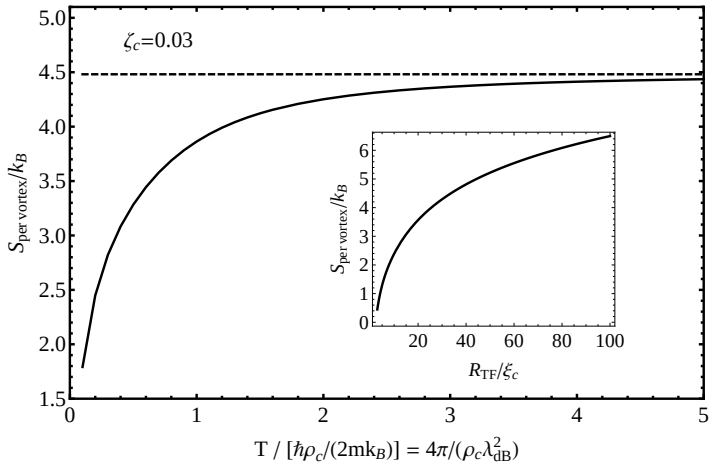

Fig. 4 The entropy per vortex is shown as a function of the temperature, related to the phase space density. The dashed horizontal line shows the temperature independent estimate $S_0 = -4k_B log(\zeta_c/r_c)$. These results were computed for $\zeta_c = 0.03$. In the inset, the dependence of the entropy per vortex on the ratio $R_{TF}/\xi_c = 1/\zeta_c$ is shown for the temperature independent estimate: as the cloud size (measured in healing lengths) grows, the entropy grows.

in a homogeneous condensate of size R_{TF}, there are ξ_c^2/R_{TF}^2 possible locations, so that the entropy becomes $S = -2k_B \log(\zeta_c^2)$. Then, the free energy $F = E - TS$ becomes zero at $T_{KT,0} = E_b^{KT}/S = \pi$ in our units. In SI units this becomes $T_{KT,0} = (\pi/2)\hbar\rho_c/(mk_B)$.

Having found that the finite size and inhomogeneity change the binding energy, we now still need to find the effect on the entropy in order to derive how large the shift in the Kosterlitz-Thouless temperature will be. Now, the vortices feel a potential landscape, and this provides additional information as to where the vortices are expected to be positioned, thus reducing the entropy.

In particular, if we have a potential landscape $U(\mathbf{r})$, we can assign a Boltzmann-type probability to the vortex location via:

$$P(\mathbf{r}) \propto \exp\{-U(\mathbf{r})/(k_B T)\}. \tag{18}$$

The probability distribution is normalized by the partition function,

$$\mathscr{Z} = \int \frac{d^2\mathbf{r}}{\pi\xi(\mathbf{r})^2} \exp\{-U(\mathbf{r})/(k_B T)\} \tag{19}$$

$$\Rightarrow \int \frac{d^2\mathbf{r}}{\pi\xi(\mathbf{r})^2} P(\mathbf{r}) = 1 \text{ for } P(\mathbf{r}) = \frac{1}{\mathscr{Z}} e^{-U(\mathbf{r})/(k_B T)}. \tag{20}$$

The coarse-grainedness due to the size of the vortex core is taken into the integration measure, and considered as a positional density of states. If there is no potential landscape, $U(\mathbf{r})$ =constant, then also $\xi = \xi_c$ is constant and the integral over the Thomas-Fermi disc becomes $(R_{TF}/\xi_c)^2$. In that case, we obtain again

$S = -2k_B \log(\zeta_c^2)$. In the inhomogeneous case, we calculate the entropy using Shannon's formula

$$S = \int \frac{d^2\mathbf{r}}{\pi\xi(\mathbf{r})^2} P(\mathbf{r}) \log[P(\mathbf{r})], \tag{21}$$

or, equivalently, using the thermodynamic relation between entropy and partition sum,

$$S = k_B \left(T \frac{\partial \log(\mathscr{Z})}{\partial T} + \log(\mathscr{Z}) \right). \tag{22}$$

The result, using the kinetic energy of the superfluid velocity field as the potential landscape for a single vortex, is shown in figure 4. The short dashed line in this figure is the result of a simpler estimate, where we use that the effective radius for the cloud in which we can position the vortices is not given by R_{TF}, but by r_c. Vortices outside this dissociation radius escape the cloud. This corresponds to estimating the entropy by

$$S \approx -4k_B log(\zeta_c / r_c). \tag{23}$$

We find that this estimate, based on the dissociation radius, is fairly good at temperatures $T > 1$ in our units. The inset of figure 4 shows how the entropy per vortex (calculated with the potential landscape) scales with R_{TF}/ξ_c.

At this point, it is useful to note that the temperature in the units used in this paper, is equivalent to $4\pi/(\rho_c \lambda_{dB}^2)$, where λ_{dB} is the De Broglie wavelength. The onset of superfluidity can be characterized equally well by the Kosterlitz-Thouless temperature as by the critical value of the phase space density $\rho_c \lambda_{dB}^2$ required to reach the superfluid phase. The advantage of using the phase space density is that it is a dimensionless quantity. For the uniform 2D bose gas, the KT transition occurs at $(\rho_c \lambda_{dB}^2)_{KT} = 4$. In the experiment a value $(\rho_c \lambda_{dB}^2)_{exp} = 6.0 \pm 1.5$ was found[6].

In order to find the critical value of the phase space density for the inhomogeneous, confined condensate, we solve

$$T_{KT} S(\zeta_c, T_{KT}) = E_b(\zeta_c), \tag{24}$$

with the binding energy (as a function of ζ_c) given by expression (16) and the entropy (as a function of both ζ_c and T) calculated from expression (22). The solution T_{KT} is then rewritten as a phase space density, as outlined in the previous paragraph. The result is shown in figure 5, as the full curve. The point with the error bar is the experimental result[6]. We find that the result of the present calculation, $\rho_c \lambda_{dB}^2 = 5.5$, agrees better with the experiment than the value $(\rho_c \lambda_{dB}^2)_{KT} = 4$ that one obtains using the theory for a uniform 2D Bose gas.

The remaining curves illustrate the effects of different approximations. To obtain the long dashed curve, we still calculate the binding energy using the GP kinetic energy of the superflow, but we use the approximate expression (23) for the entropy. The dash-dotted curve, in addition, also approximates the binding energy by E_b^{magn}, expression (17). From this we again conclude that a description based on Magnus forces acting on point vortices can qualitatively bring into account the inhomogeneity, but fails quantitatively. This suggests that in addition to the condensate inhomogeneity, the vortex core size is still too large in comparison to the cloud radius to be ignored.

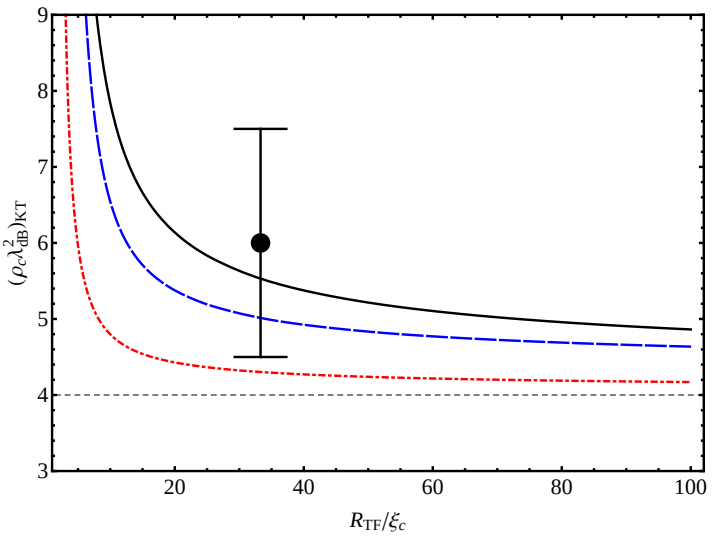

Fig. 5 (Color online) The phase space density corresponding to the Kosterlitz-Thouless transition is shown as a function of R_{TF}/ξ_c, for different levels of approximation, and compared to the experimental result [6] (point with error bar). The short dashed horizontal line is the KT result for the uniform 2D Bose gas, the other curves take into account the inhomogeneity of the trapped cloud. The full curve gives the result using the GP energy functional to obtain the binding energy as well as the entropy. The long dashed curve approximates the entropy through an effective cloud radius. The dash-dotted curve also approximates the binding energy by calculating it from the Magnus forces for point vortices.

5 Conclusion

The Kosterlitz-Thouless phenomenological argument is originally set up in the context of a uniform 2D Bose gas for which the healing length can be neglected in comparison with the size of the cloud. Here, we extend the argument to the case of an inhomogeneous atomic cloud where in addition the vortex core size can no longer be neglected with the cloud size. Both the binding energy of vortex-antivortex pairs and the entropy per vortex are affected. The former is reduced, as the vortex does not need to be removed all the way to the edge of the cloud in order for the vortex-antivortex molecule to dissociate: the image vortices help the unbinding of the vortex-antivortex pair. The entropy is also reduced, albeit to a lesser extent, because the inhomogeneity provides information on the expected vortex positions. Comparing the binding energy and the entropic contribution to the free energy allows again to derive a Kosterlitz-Thouless temperature, which is reduced with respect to that of the homogeneous case. The current extension of the KT phenomenological argument gives a good agreement with a recent experiment in trapped atomic Bose gases. Investigating different levels of approximation, we find that a description based on Magnus forces on point vortices is too crude to quantitatively capture the change in KT temperature, whereas a derivation using the GP kinetic energy of superfluid flow gives quantitative agreement.

Acknowledgements The authors acknowlegde financial support by the Fund for Scientific Research - Flanders, through project nrs G011512N and G011912N. E. Vermeyen acknowledges support in the form of a Ph. D. fellowship of the Research Foundation - Flanders (FWO).

References

1. A. Griffin, D.W. Snoke and S. Stringari, eds., *Bose-Einstein condensation* (Cambridge University Press, Cambridge, UK, 1996).
2. V.L. Berezinskii, *Sov. Phys. JETP* **32**, 493, (1971).
3. J.M. Kosterlitz and D.J. Thouless, *J. Phys. C* **6**, 1181, (1973).
4. J.M. Kosterlitz, *J. Phys. C* **7**, 1046, (1974).
5. D.R. Nelson and J.M. Kosterlitz, *Phys. Rev. Lett.* **39**, 1201, (1977).
6. Z. Hadzibabic, P. Krüger, M. Cheneau, B. Battelier, and J. Dalibard, *Nature* **441**, 1118, (2006).
7. Z. Hadzibabic, P. Krüger, M. Cheneau, S.P. Rath, J. Dalibard, *New J. Phys.* **10**, 045006 (2008).
8. M. Holzmann and W. Krauth, *Phys. Rev. Lett.* **100**, 190402, (2008).
9. R. N. Bisset, M. J. Davis, T. P. Simula, and P. B. Blakie, *Phys. Rev. A* **79**, 033626, (2009).
10. S.P. Rath, T. Yefsah, K.J. Guenter, M. Cheneau, R. Desbuquois, M. Holzmann, W. Krauth, and Jean Dalibard, *Phys. Rev. A* **82**, 013609, (2010).
11. D. Gallucci, S. P. Cockburn, and N. P. Proukakis, *Phys. Rev. A* **86**, 013627, (2012).
12. N. Prokofev, O. Ruebenacker, and B. Svistunov, *Phys. Rev. Lett.* **87**, 270402 (2001).
13. S. Sachdev and E. Demler, *Phys. Rev. B* **69**, 144504 (2004).
14. C. J. Pethick and H. Smith, it Bose-Einstein Condensation in Dilute Gases (Cambridge University Press, Cambridge, UK, 2002).